



The value of neck adipose tissue as a predictor for metabolic risk in health and type 2 diabetes

Emily Cresswell^{a,b}, Nicolas Basty^c, Naeimeh Atabaki Pashar^{a,d}, Fredrik Karpe^{a,e,*}, Katherine E. Pinnick^{a,*}

^a Oxford Centre for Diabetes, Endocrinology and Metabolism, University of Oxford, Oxford, UK

^b The Kennedy Institute of Rheumatology, University of Oxford, Oxford, UK

^c Research Centre for Optimal Health, University of Westminster, London, UK

^d Genetic and Molecular Epidemiology Unit, Lund University Diabetes Centre, Department of Clinical Science, Lund University, Malmö, Sweden

^e NIHR Oxford Biomedical Research Centre, OUH Foundation Trust, Oxford, UK

ARTICLE INFO

Keywords:

Neck
Adipose tissue
Cardiometabolic health
Type 2 diabetes mellitus
Fat distribution
Imaging

ABSTRACT

Upper-body adiposity is adversely associated with metabolic health whereas the opposite is observed for the lower-body. The neck is a unique upper-body fat depot in adult humans, housing thermogenic brown adipose tissue (BAT), which is increasingly recognised to influence whole-body metabolic health. Loss of BAT, concurrent with replacement by white adipose tissue (WAT), may contribute to metabolic disease, and specific accumulation of neck fat is seen in certain conditions accompanied by adverse metabolic consequences. Yet, few studies have investigated the relationships between neck fat mass (NFM) and cardiometabolic risk, and the influence of sex and metabolic status. Typically, neck circumference (NC) is used as a proxy for neck fat, without considering other determinants of NC, including variability in neck lean mass. In this study we develop and validate novel methods to quantify NFM using dual x-ray absorptiometry (DEXA) imaging, and subsequently investigate the associations of NFM with metabolic biomarkers across approximately 7000 subjects from the Oxford BioBank. NFM correlated with systemic insulin resistance (Homeostatic Model Assessment for Insulin Resistance; HOMA-IR), low-grade inflammation (plasma high-sensitivity C-Reactive Protein; hsCRP), and metabolic markers of adipose tissue function (plasma triglycerides and non-esterified fatty acids; NEFA). NFM was higher in men than women, higher in type 2 diabetes mellitus compared with non-diabetes, after adjustment for total body fat, and also associated with overall cardiovascular disease risk (calculated QRISK3 score). This study describes the development of methods for accurate determination of NFM at scale and suggests a specific relationship between NFM and adverse metabolic health.

1. Introduction

Human fat distribution influences whole body metabolism through the differential functions of discrete fat depots, and thereby affects cardiovascular health [1]. Neck fat accumulation is seen in certain adiposity redistribution syndromes, including Cushing's disease [2], partial lipodystrophies [3,4] and obesity hypoventilation syndrome [5], which all show robust associations with insulin resistance and metabolic

abnormalities. Recent interest in neck fat has grown succeeding the serendipitous rediscovery of adult brown adipose tissue (BAT) following [¹⁸F]-labelled 2-deoxyglucose positron emission tomography, which revealed a region across the anterior neck and supraclavicular boundaries displaying high glucose uptake and metabolically active tissue.

In obesity, there is concurrent regression of BAT and replacement with white adipose tissue (WAT) [6–9], which has been hypothesized to contribute to metabolic complications in obesity. BAT whitening likely

Abbreviations: BAT, Brown Adipose Tissue; BMI, Body Mass Index; BMP4, Bone Morphogenic Protein 4; DEXA, Dual Energy X-ray Absorptiometry; DNA, Deoxyribonucleic Acid; FMI, Fat Mass Index; GWAS, Genome Wide Association Study; HDL, High-Density Lipoprotein; HOMA-IR, Homeostatic Model Assessment for Insulin Resistance; hsCRP, High-Sensitivity C-Reactive Protein; NAT, Neck Adipose Tissue; NC, Neck Circumference; ND, Neck Diameter; NEFA, Non-Esterified Fatty Acid; NFM, Neck Fat Mass; ROI, Region Of Interest; SAT, Subcutaneous Adipose Tissue; SBP, Systolic Blood Pressure; SNP, Single Nucleotide Polymorphism; T2DM, Type 2 Diabetes Mellitus; TG, Triglyceride; VAT, Visceral Adipose Tissue; VFM, Visceral Fat Mass; WAT, White Adipose Tissue; WC, Waist Circumference.

* Corresponding authors at: Oxford Centre for Diabetes, Endocrinology and Metabolism, University of Oxford, Oxford, UK.

E-mail addresses: fredrik.karpe@ocdem.ox.ac.uk (F. Karpe), katherine.pinnick@ocdem.ox.ac.uk (K.E. Pinnick).

<https://doi.org/10.1016/j.bcp.2024.116171>

Received 31 October 2023; Received in revised form 14 March 2024; Accepted 26 March 2024

Available online 27 March 2024

0006-2952/© 2024 The Authors. Published by Elsevier Inc. This is an open access article under the CC BY license (<http://creativecommons.org/licenses/by/4.0/>).

Table 1

Cohort Summary Data. Mean and standard deviation values for common metabolically relevant variables. Data are subdivided by sex and T2DM status. BMI = body mass index (weight (kg) / height (m)²), HOMA-IR = Homeostatic Model Assessment for Insulin Resistance (glucose (mmol/L) x insulin (mU/L) / 22.5); LDL = low-density lipoprotein; HDL = high-density lipoprotein; TG = triglyceride; NEFA = non-esterified fatty acid; hsCRP = high-sensitivity C-reactive protein.

Variable	Sex	No Diabetes		T2DM	
		Mean ± SD	N	Mean ± SD	N
Age (y)	Male	43.36 ± 8.60	2586	60.68 ± 10.37	487
	Female	42.68 ± 7.81	3568	59.47 ± 11.15	314
BMI (kg/m ²)	Male	26.60 ± 4.11	2584	30.58 ± 5.27	480
	Female	25.45 ± 5.07	3562	32.34 ± 6.37	310
Neck Fat Mass (g)	Male	301.14 ± 155.29	2586	497.82 ± 223.98	487
	Female	228.16 ± 128.49	3568	445.99 ± 199.74	314
Neck Diameter (cm)	Male	12.65 ± 1.22	2577	14.49 ± 1.70	408
	Female	11.47 ± 1.19	3559	14.20 ± 1.91	258
HOMA-IR	Male	3.24 ± 2.27	2543	9.76 ± 7.48	30
	Female	2.65 ± 1.64	3516	10.97 ± 8.55	10
LDL-cholesterol (mmol/L)	Male	3.42 ± 0.87	2561	3.55 ± 1.00	30
	Female	3.09 ± 0.82	3566	4.13 ± 1.17	10
HDL-cholesterol (mmol/L)	Male	1.20 ± 0.32	2584	1.03 ± 0.20	31
	Female	1.52 ± 0.39	3568	1.55 ± 1.66	11
TG (mmol/L)	Male	1.34 ± 0.86	2586	1.56 ± 0.87	487
	Female	0.94 ± 0.48	3568	1.51 ± 0.72	314
Glycerol (μmol/L)	Male	42.56 ± 28.29	2580	70.43 ± 55.15	31
	Female	61.56 ± 35.3	3561	73.62 ± 19.08	10
NEFA (μmol/L)	Male	427.55 ± 202.27	2586	600.41 ± 261.71	487
	Female	510.17 ± 240.24	3568	728.84 ± 279.66	314
hsCRP (mg/L)	Male	1.70 ± 5.32	2579	3.56 ± 5.24	31
	Female	1.81 ± 3.99	3558	6.05 ± 5.34	10

enlarges neck fat mass (NFM) due to the greater lipid storage capacity of WAT, thus increasing neck circumference (NC). Notably, robust relationships have been reported between NC and cardiometabolic risk factors including measures of blood pressure, glucose homeostasis, cholesterol, triglycerides, as well as standard anthropometric variables such as waist circumference (WC) and body mass index (BMI), and metabolic disease including type 2 diabetes mellitus (T2DM) [10–16]. Neck adiposity has been credited as a reliable index of upper-body fat [17], and is closely associated with abdominal adiposity and central obesity [18,19]. However, after adjusting for total fat mass, NC also shows independent associations with biomarkers including insulin resistance, triglycerides and cholesterol, with NC outperforming WC in some studies [10,20,21].

It has been suggested that neck adipose tissue (NAT), with its proximity to the carotid blood vessels could play a role in regulating vascular tone through the secretion of various adipokines and vasomodulatory factors [22,23]. Indeed, NC has been associated with arterial stiffness [24], carotid intima-media thickness [25], as well as cardiovascular outcomes [26], remaining significant even after correcting for visceral adipose tissue (VAT) mass. These data suggest that NAT, as an upper-body fat depot, could play an independent role in obesity-related metabolic dysfunction.

Others have suggested that the unique role that neck fat plays in metabolic health arises from its ability to release non-esterified fatty acids (NEFA) [27]. Upper-body adiposity has been linked to raised postprandial NEFA originating from non-visceral upper-body fat, such as the neck [28,29]. The increased flux of NEFA from the neck to the liver may contribute to excess triglyceride accumulation and steatotic liver disease [30,31].

Recording NC with a tape measure has been a typically favoured method because of its ease of implementation, yet this does not distinguish between fat and lean mass in the neck. A study that has investigated NAT volume, however, observed stronger relationships between NAT volume and metabolic parameters, as compared to NC [32], highlighting the need to evaluate alternative methods to quantify neck adiposity besides NC. Further to this, the evidence relating specifically to the association between NFM and obesity, sex and metabolic status is limited, despite its established influences on mortality and T2DM [33]. This is likely due to the limited availability of NFM data; the neck isn't a standard region for dual x-ray absorptiometry (DEXA) body composition outputs, and manually extracting NFM measurements from DEXA scans is a very time-consuming process. Thus far, machine learning methods have not been investigated as a tool for automated measurement of NFM. This study aims to establish and validate a novel method to estimate NFM from existing DEXA scans using convolutional neural networks, a class of machine learning that has established itself as the go-to methodology in computer vision and is frequently used in medical imaging studies for tasks such as disease classification and segmentation [34]. We applied this automated pipeline to assess NFM in a large cohort of people with and without T2DM, then investigated NFM in relation to relevant cardiometabolic and anthropometric indicators.

2. Materials and methods

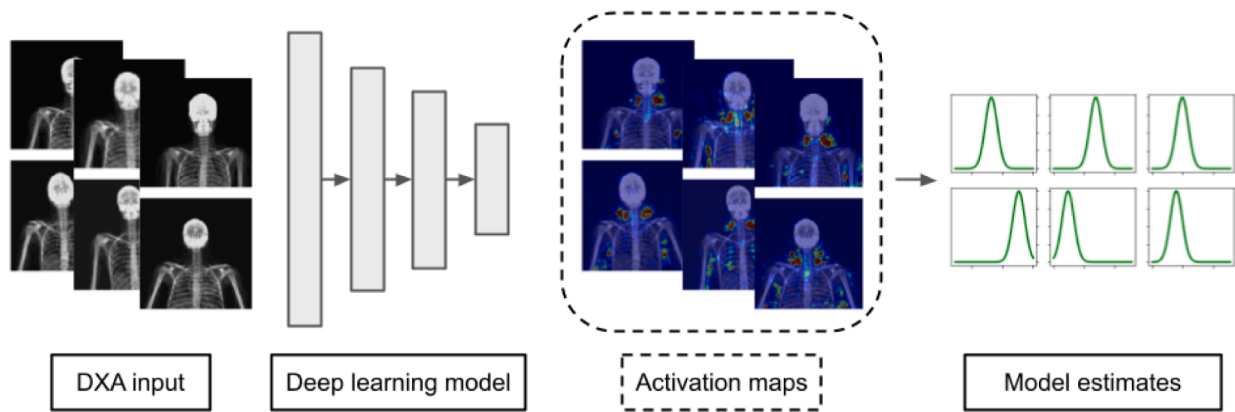
2.1. Study population

The Oxford BioBank was utilised for all data acquisition [35]. This is a population-based bioresource, containing cardiovascular- and obesity-related phenotypes including biomarkers pertaining to fasting plasma biochemistry, genetics, anthropometrics and body composition (e.g. regional fat mass values) as assessed using DEXA scanning of European ancestry individuals living in Oxfordshire. We utilised 6955 DEXA scans to quantify NFM across individuals with and without T2DM. Descriptive statistics for common biomarkers including mean values and standard deviations were computed, partitioning by sex and T2DM status, and are presented in Table 1. Ethical approval was granted by the Oxfordshire Clinical Research Ethics Committee (08/H0606/107 + 5) and all participants provided informed consent.

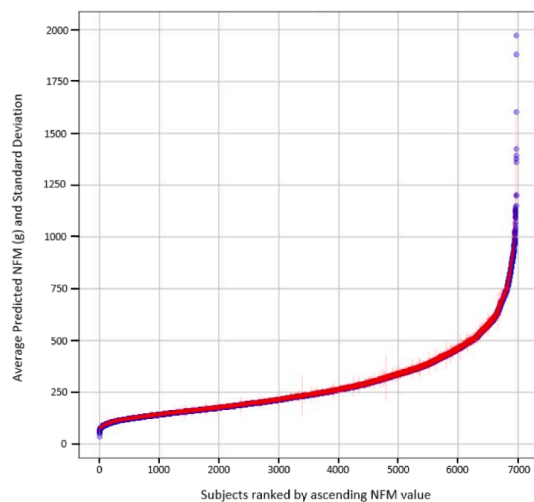
2.2. Acquiring ROI and NFM data

Regional fat mass can be reliably estimated using DEXA scanning, which utilises x-rays to quantify bone mineral density, as well as body composition parameters such as lean and adipose tissue. Quantification, however, largely relies on proprietary methodologies for analyses performed within the scanner software, which are inaccessible to users and usually not made available. Custom analysis for non-standardly defined regions, such as the neck, frequently requires manual input to select regions of interest on individual scans, which makes working with large DEXA databases impractical. To this end, we designed an automated pipeline utilising DEXA images for NFM estimation based on convolutional neural networks. Detailed methodology are available from Cresswell et al [36], but brief methods are summarised below and in Fig. 1a.

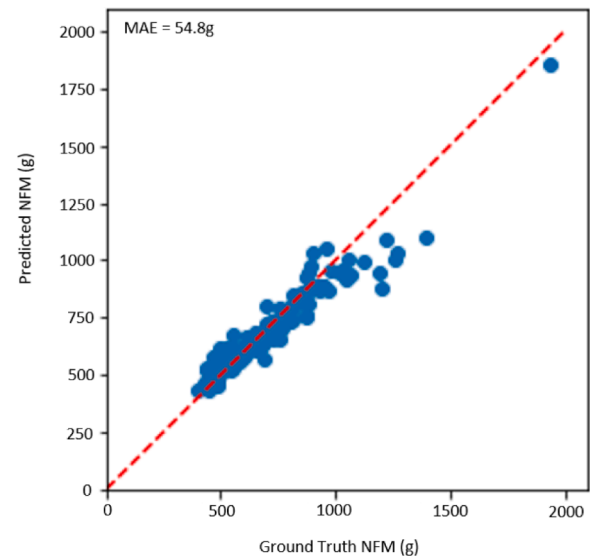
We used DEXA images from 495 participants from the Oxford Bio-Bank, representing a wide range of BMI values, to train and validate a deep learning model for placement of the neck region of interest (ROI), to estimate neck diameter. To get training data for the ROI placement neural network, for each DEXA scan, four points were placed at each corner of the ROI. The ROI was constructed using both skeletal and soft tissue scans to identify predefined anatomical landmarks. The height of the ROI was set at the top lung apices and the lower margins of the mandible on both the right and left sides, with the width of the ROI being adjusted to suit neck diameter. From here, we created a pipeline to accurately perform ROI placement, training a U-net using 400 images



a



b



c

Fig. 1. NFM estimation pipeline and validation. a) DEXA images were used as input to the NFM estimation model which produces probabilities of neck fat measurement estimates for each subject. An ensemble average of 10 models per measurement is used to make predictions more robust. Model activation maps are shown as an intermediate step, to enable visual assurance that the trained models are indeed focusing on the neck region. b) NFM average estimations and standard deviation across 10 models for NFM ($n = 6955$) c) Validation scatterplot. Ground truth compared to estimated values for NFM ($n = 143$). Mean absolute error (MAE) = 54.8 g.

and the corresponding co-ordinates obtained from these manually placed ROIs [36]. We trained a second model to quantify NFM using image regression based on a study performing brain age estimation and our previous work [36,37]. For this, we used DEXA images from 1143 participants, where we enriched the cohort to improve model performance, as the ROI work predates the NFM estimation work. To obtain NFM values used as ground truth in training the regression network, the scanner software gave a value for NFM based on the constructed ROI for each participant. To estimate NFM, we trained a model using only the top half of DEXA scan images. Output data for both models were compared to manual annotations to validate the model ROI placements and NFM estimation, and quantified using mean absolute error (the sum of absolute errors between true and estimated values divided by the sample size). We evaluated the ROI placement model and NFM model based on held-out testing data that were not used in model design or training ($n = 95$, $n = 143$, respectively). The model was then applied to the remaining available scans in the Oxford BioBank.

2.3. Neck skinfold and circumference measurements

Measurements for neck skinfold and circumference were taken with participants standing or sitting, with the head straight, shoulders relaxed and looking at a distant object without bending the neck. The vertical midpoint between the angle of the mandible and the clavicle was located for use as the height of the measurement site for NC and neck skinfold. NC was measured by taking a tape measure taught around the neck, traversing the identified midpoints. At the same midpoint, skinfold was measured, in mm, 3 times using skin calipers, and the average value from these was taken.

2.4. NFM adjustment

NFM is strongly related to total body fat mass (men: $r = 0.80$, $p < 0.00001$, $n = 2586$; women: $r = 0.82$, $p < 0.00001$, $n = 3568$). Thus it was important to establish an indicator for higher or lower NFM

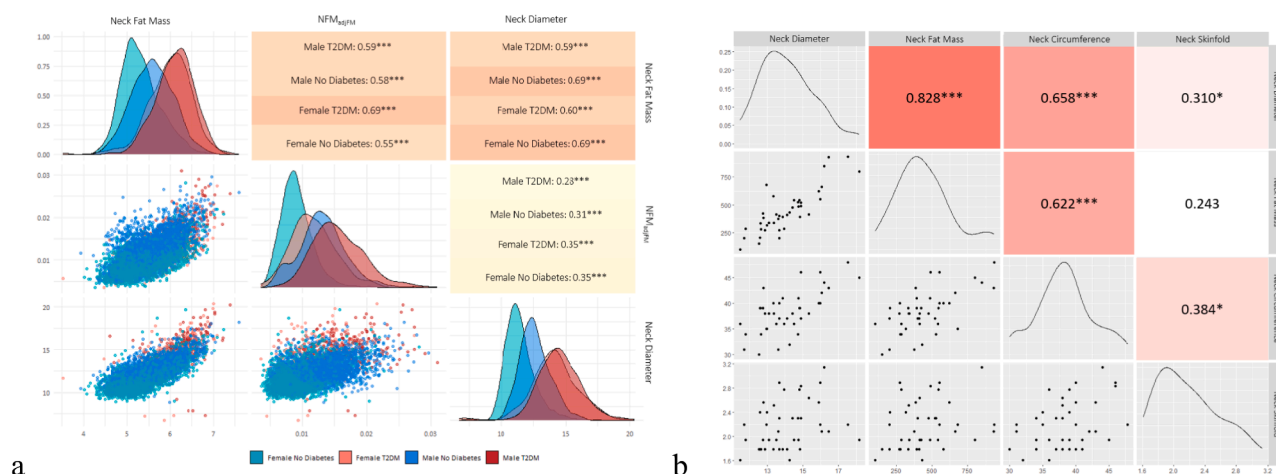


Fig. 2. Associations between neck fat parameters. NFM units are in grams, NFMadjFM units are the proportion of NFM to total fat mass, and the remaining variables are measured in centimetres. a) Correlations between predicted ND, NFMadjFM, and NFM. Data is stratified and coloured by subgroup in scattergraph and density plots ($n = 6934$). NFM values are log-transformed. Pearson correlation co-efficients are coloured by strength of association and significance is indicated by asterisks (* $p < 0.05$; ** $p < 0.01$; *** $p < 0.001$). b) Correlations between predicted neck fat parameters (NFM, ND), and actual measurements (NC, neck skinfold). Actual neck fat measurements were taken from a subset of the T2DM group ($n = 41$), as detailed in Section 2.3. Scatterplots and density plots for each variable are displayed on the lower-left and central line of the grid respectively, and Pearson correlation co-efficients are displayed in the upper-right panel, coloured by strength of association. Neck skinfold values are log-transformed. Asterisks indicate significance of association (* $p < 0.05$; ** $p < 0.01$; *** $p < 0.001$).

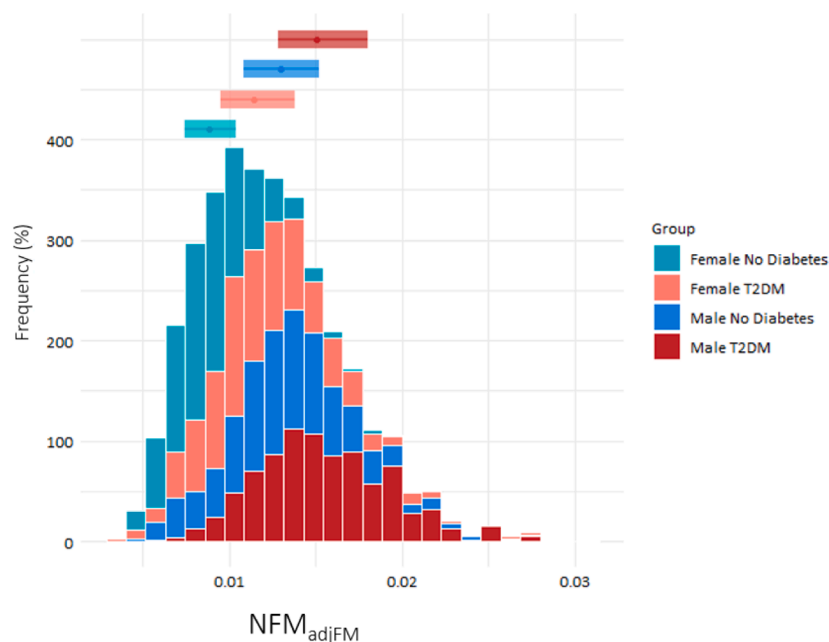


Fig. 3. Distribution of NFMadjFM stratified by sex and T2DM. Relative frequency histogram, illustrating differences in NFMadjFM. Data are stratified and coloured by subgroup. Horizontal bars representing the interquartile range for each group are shown above the histogram, and the median values are represented by the point within the bar ($n = 6394$).

abundance in relation to total body fat. We therefore divided NFM by total fat mass to generate a value for adjusted NFM (NFMadjFM), giving a value for relative regional neck fat distribution. The same calculation was conducted for visceral fat mass (VFM), to establish a relative value for visceral adiposity (VFMadjFM). All values for regional adipose masses were taken from DEXA-based measurement.

2.5. Correlation analyses

NAT measures were correlated with variables of interest using Pearson's correlation co-efficient tests. Variables were log-transformed if normality, tested using the Shapiro–Wilk test, was not met. Fat mass index (FMI) was calculated by dividing total fat mass (kg) by height (m) squared. Body mass index (BMI) was calculated by dividing total body mass (kg) by height (m) squared. Cardiovascular risk was calculated using a broad range of parameters that have been previously

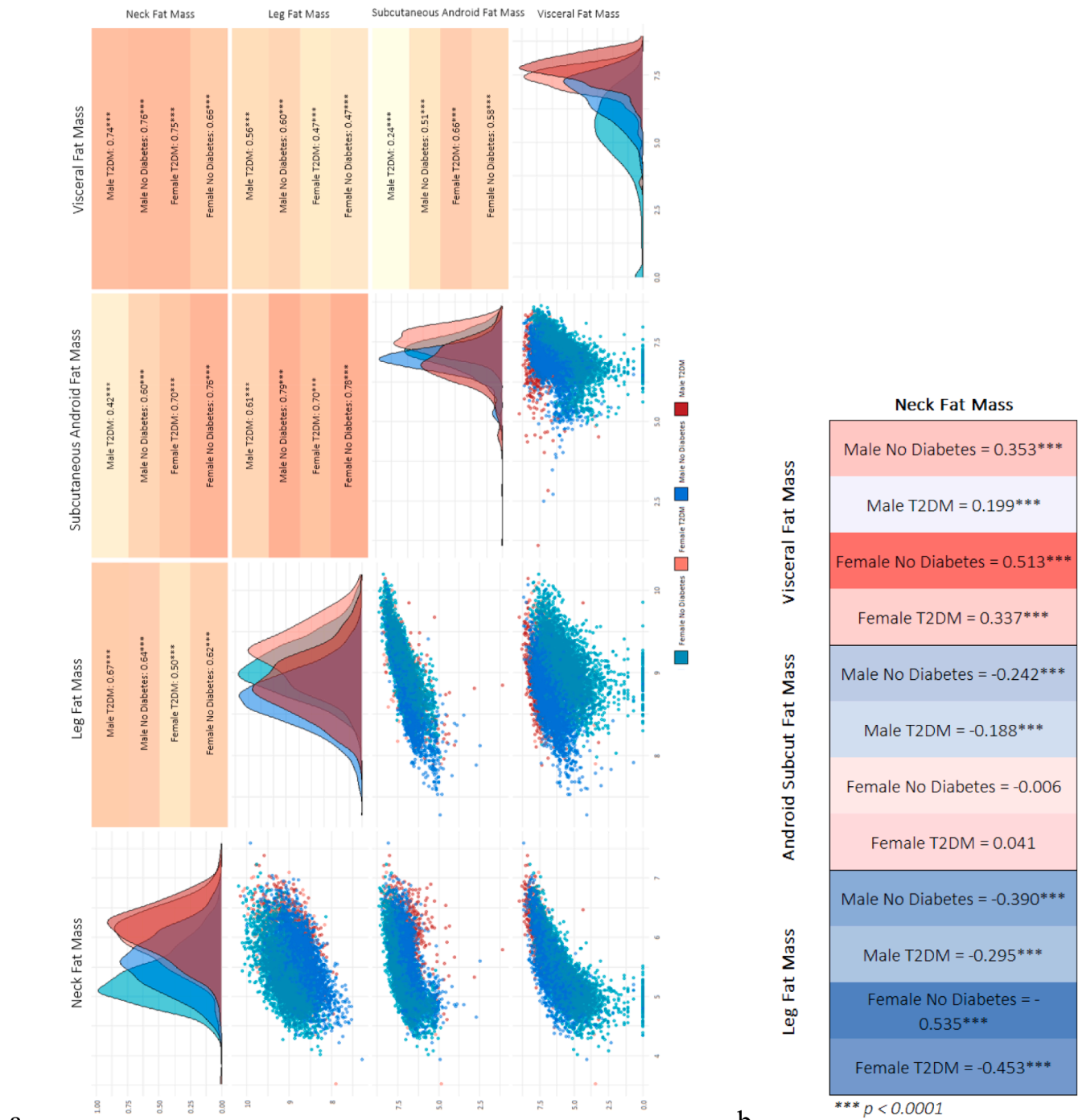


Fig. 4. NFM associations with other adipose depot masses. a) Correlations between NFM and other fat depots ($n = 6934$). Scattergraphs and density plots are stratified and coloured by subgroup. Pearson correlation co-efficients are displayed in the upper-right panel, with asterisks indicating the significance of associations (* $p < 0.05$; ** $p < 0.01$; *** $p < 0.001$). b) Partial correlation analysis between NFM and other adipose tissue masses, controlling for total fat mass. Analyses are stratified by group, and coloured by strength of association ($n = 6934$). Asterisks indicate the significance of associations (* $p < 0.01$; ** $p < 0.001$; *** $p < 0.0001$).

incorporated into a validated model named QRISK3 [38], which is used clinically to calculate risk of cardiovascular events within the next 10 years. Factors incorporated into this score include: presence of atrial fibrillation, erectile dysfunction, migraines, rheumatoid arthritis, chronic kidney disease, severe mental illness, systemic lupus erythematosus, type 1 diabetes and T2DM; taking medications including atypical antipsychotics, corticosteroids and high blood pressure treatment; weight; height; ethnic origin; angina; total cholesterol to high-density lipoprotein (HDL)-cholesterol ratio; systolic blood pressure; age; sex and smoker status. In the Oxford BioBank, complete data were

available for the presence of T2DM; blood pressure treatment; weight; height; ethnic origin; total cholesterol to HDL-cholesterol ratio; systolic blood pressure; age; sex and smoker status, while self-reported data were relied upon for the remaining QRISK3 components. QRISK3 score was then calculated using these parameters, input into the QRISK3 R package (available at: <https://github.com/YanLiUK/QRISK3>). Statistical analyses were conducted using RStudio (version 2023.06.1 + 524) and R (version 4.3.1). An unpaired student's t -test analysis was used to compare NFM measures across groups.

Table 2

Associations between common body mass metrics and neck fat mass. Data are divided by sex and T2DM status ($n = 6934$). BMI = body mass index (weight (kg) / height (m)²); FMI = fat mass index (total fat mass (kg) / height (m)²).

Cohort	BMI	Total Fat Mass	Total Lean Mass	FMI
Male No Diabetes	0.75	0.80	0.30	0.80
Female No Diabetes	0.80	0.82	0.36	0.82
Male T2DM	0.78	0.82	0.45	0.82
Female T2DM	0.76	0.79	0.52	0.79

Note: Pearson's correlation co-efficients; $p < 0.00001$ for all displayed associations.

2.6. Genetic analysis

Genetic single nucleotide polymorphism (SNP) data were sourced through existing analyses from the Oxford BioBank, as detailed in Karpe et al [35]. Methods are briefly summarised below. For isolation of genomic DNA, 3 x 5 ml whole blood aliquots were collected for each participant, before freezing at -80°C . Whole genome SNP arrays were generated using Affymetrix UK Biobank Axiom Array chips (now part of ThermoFisher Scientific, Waltham, MA, United States). Fourteen SNPs that have shown significant association with NC from previous studies were selected [39–41] to conduct a genetic association analysis with NFM and NC using measurements available in the Oxford BioBank. Individuals with complete genetic and neck fat data were selected ($n = 4518$) and those with BMI > 50 or BMI < 18 were excluded, leaving 4494 individuals (1942 male, 2552 female) for input data. All the phenotypes were first adjusted for sex, age, and the first 4 genetic principal components, and then the residuals from the fitting models were inverse-normalised and used in association with each SNP. For sex-separated analyses, phenotypes were adjusted for age, and the first 4 genetic principal components.

3. Results

3.1. Validation of machine learning-estimated neck measurements

DEXA scans were fed into a machine learning model, firstly to delineate the ROI based on anatomical landmarks and subsequently to estimate NFM (Fig. 1a). The output data from the machine learning-based networks were compared to manually quantified neck parameters (NFM and neck diameter) to validate the model estimations for ROI placement and NFM estimation. Analysing the ROI placement showed that the network could estimate the four neck boundary landmarks with an accuracy of less than 3 pixels (< 6.9 mm). The plotted population distribution for estimated NFM averaged over 10 models showed consistently small standard deviations across a wide range of estimation values, demonstrating that the model could be applied across a wide NFM range without sacrificing estimation abilities (Fig. 1b). Furthermore, when NFM estimations were compared to ground truth values in a held-out testing dataset ($n = 143$), we saw a strong linear correlation (Fig. 1c) and a mean absolute error value of 54.8 g, indicating a high performance accuracy from the model. Activation maps then confirmed that the network was focusing on the neck region to make its estimates (Fig. 1a). The model highlighted areas in red (generally showing the neck) that it was using to make its estimates, and areas in blue (showing regions outside the neck, and image background) which were not prioritised in its decision making. Neck diameter (ND) values were calculated based on the distance between estimated landmarks of the ROI model, whereas NFM was estimated directly from the upper half of the DEXA image (Fig. 1a). Significant and strong correlations between ND and NFM were observed (Fig. 2a & b). Assuming that the neck is cylindrical, ND will be linearly associated with NC, allowing us to relate our findings to the existing literature, where NC is frequently used as a proxy measurement for NFM. We also investigated the relationship

between directly measured NC or neck skinfold measurements with estimated NFM in a small subset of people ($n = 41$). NC, directly measured by tape measure, showed a weaker correlation with NFM than for the estimated ND value, presumably because of the variability of human measurement when quantifying NC. Neck skinfold poorly reflected NFM, likely due to its basis on a single measurement in one location (Fig. 2b).

3.2. NFM in relation to sex, age and diabetes

NFMadjFMI, acted as an indicator for relative regional neck fat distribution. The stratified relative frequency histogram (Fig. 3a) showed higher NFMadjFMI in men compared to women, with the sex difference proving statistically significant when further tested with a t -test (healthy: $p < 1.0\text{e-}70$, T2DM: $p < 1.4\text{e-}36$). The histogram also revealed higher NFMadjFMI in people with T2DM compared with no diabetes, which was again statistically significant for both men and women when tested (men: $p < 6.2\text{e-}38$, women: $p < 4.6\text{e-}67$). This strongly indicates that there is a regional shift in fat distribution towards the neck occurring with T2DM. Although the T2DM population was older, no clear relationship was seen between NFM and age, while positive significant relationships were seen for VAT in the same individuals (data not shown).

3.3. NFM is associated with other fat depot masses, particularly VAT

Without controlling for total body fat, NFM correlated positively and significantly with other regional fat masses in men and women, with and without T2DM (Fig. 4a). Weaker correlations were seen between NFM and measures of subcutaneous abdominal adiposity and leg fat mass, while correlations with VFM were strong and consistent across all 4 subgroups. However, after controlling for total fat mass using partial correlations, NFM remained significantly and positively associated with VFM, while it became negatively associated with leg fat mass in all groups. In women, we observed stronger negative correlations between NFM and leg fat mass compared to males, suggesting that females show stronger regional dimorphisms in upper- versus lower-body fat expansion. Negative associations were also apparent for abdominal subcutaneous fat mass in men with and without T2DM (Fig. 4b).

3.4. NFM is associated with metabolic status

We found robust correlations between NFM and widely employed obesity metrics, such as BMI, total fat mass, and FMI, as depicted in Table 2. These correlations were consistent and significant across the subgroups, encompassing both sexes and individuals with and without T2DM. Significant relationships were also seen between NFM and total lean mass, but the association was weaker as compared to BMI, total fat mass and FMI. Stronger relationships were observed between NFM and specific measures of adiposity (total fat mass and FMI), as compared to BMI, confirming that NFM expansion may be largely paralleled by increasing adiposity, as opposed to lean mass. Without correcting for total fat mass, NFM and VFM showed positive, significant correlations of very similar strength for insulin resistance (HOMA-IR), plasma triglycerides (TG), systemic low-grade inflammation (hsCRP), blood pressure (SBP) and cholesterol in both men and women without T2DM (data not shown). When correcting for total fat mass, however, relationships between NFM and these metabolic markers weakened, despite remaining highly significant, while those for VFM stayed largely the same (Fig. 5). We used the QRISK3 algorithm to estimate overall cardiovascular risk in relation to NFMadjFMI mass and VFMadjFMI in a population without T2DM. NFMadjFMI values were used to divide individuals into deciles. QRISK3 score was then compared across these deciles, to indicate how cardiovascular risk may change with increasing relative neck adiposity. 10-year cardiovascular event risk was approximately 2-fold higher comparing the lowest NFMadjFMI decile with the

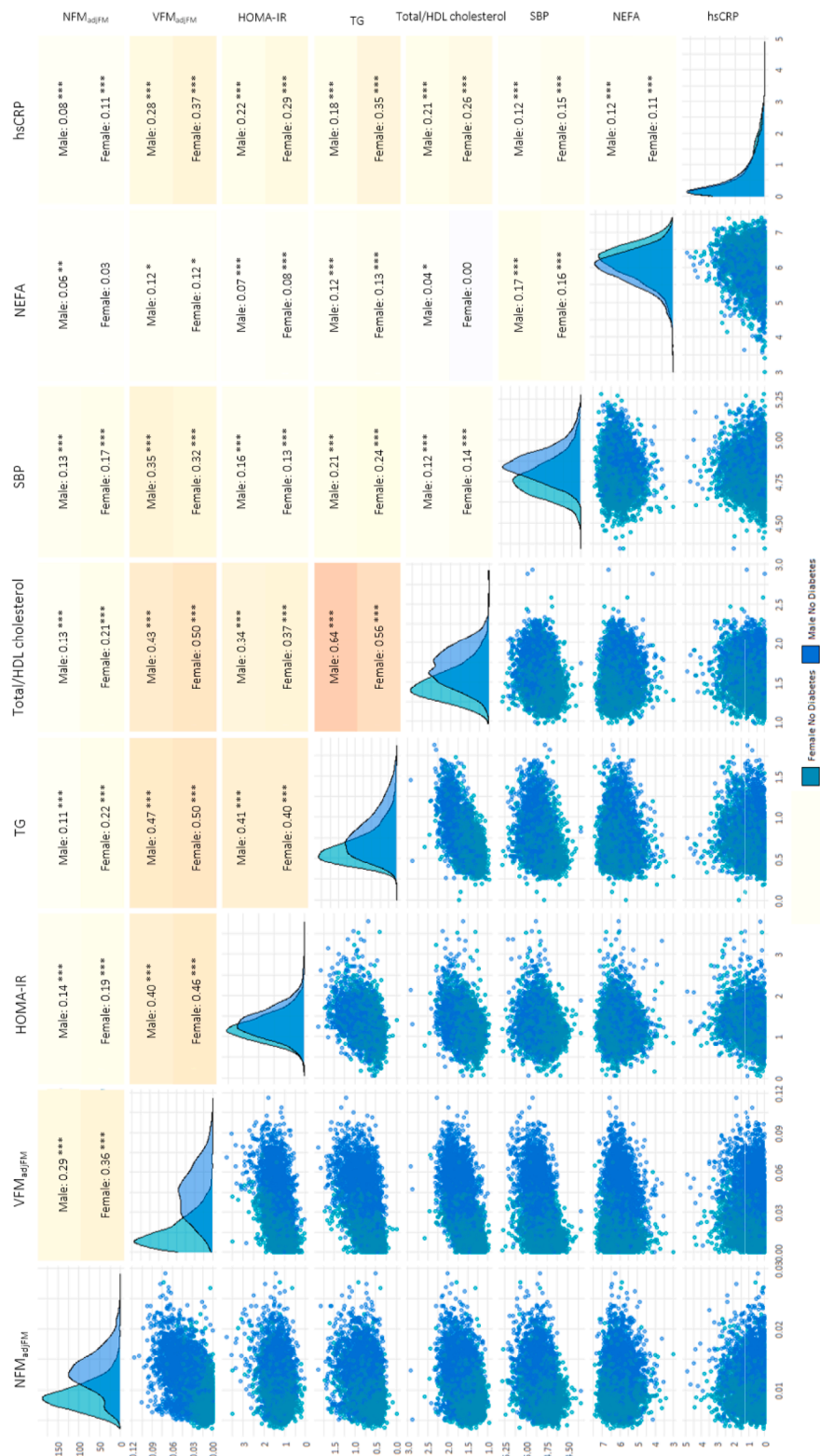


Fig. 5. Correlation between NFM_{adjFM} and relevant cardiometabolic risk variables. All values have been log-transformed. Scatterplots and density plots are stratified and coloured by sex, using the non-T2DM population. On the upper-right panel, Pearson correlation co-efficients are displayed, and boxes are coloured by strength of association. Asterisks indicate the significance of association (* $p < 0.05$; ** $p < 0.01$; *** $p < 0.001$). HOMA-IR = Homeostatic Model Assessment for Insulin Resistance (glucose (mmol/L) x insulin (mU/L) /22.5); TG = triglyceride; Total/HDL cholesterol = total cholesterol / high-density lipoprotein cholesterol; SBP = systolic blood pressure; NEFA = non-esterified fatty acid; hsCRP = high-sensitivity C-reactive protein.

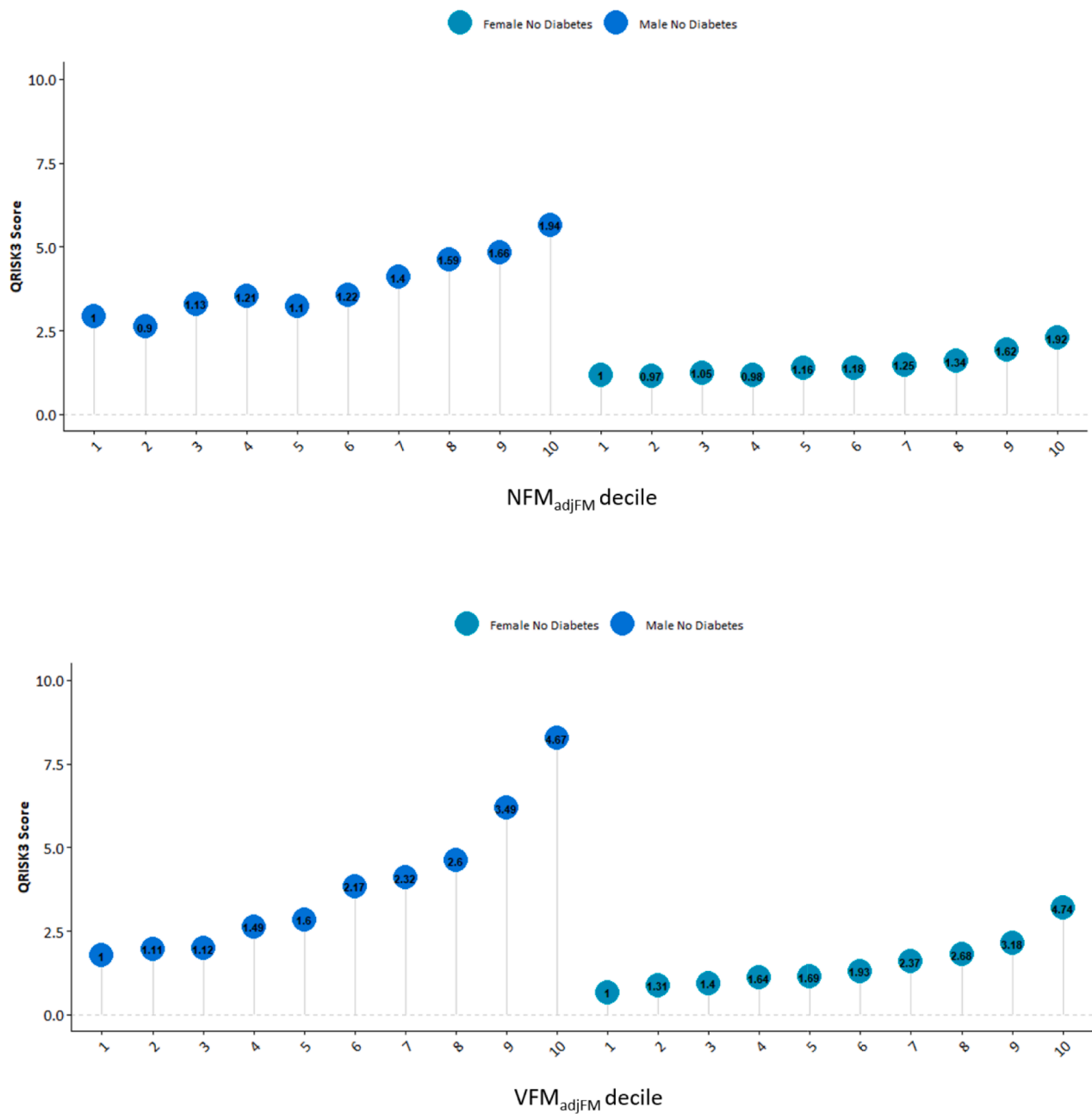


Fig. 6. QRISK3 scores, stratified by NFMadjFM and VFMadjFM. Relative differences in QRISK3 score across the deciles is captioned in the coloured bubbles, and is relative to the score of the first decile. Data are stratified and coloured by sex, using the non-T2DM groups. a) QRISK3 score stratified by NFMadjFM b) QRISK3 score stratified by VFMadjFM.

top decile in both men and women (Fig. 6), illustrating that a greater relative distribution of fat towards the neck region, independent of total adiposity, is robustly associated with multiple measures of cardiometabolic risk in a healthy population. VFMadjFM also showed a robust relationship with QRISK3 score, in both men and women, where we saw roughly 4.7-fold greater risk score when comparing the lowest and highest VFMadjFM deciles.

3.5. Neck fat genetic analysis

To establish whether our measures of neck adiposity have a genetic component, we looked at measures of NFM in association with 14 literature-driven [39–41] SNPs across the Oxford BioBank dataset (Table 3). Notably, 8 of these SNPs that had previously demonstrated

associations with NC were consistently and significantly linked with estimated NC or NFM in our dataset (as outlined in Table 4), validating the translatable utility of our data.

4. Discussion

Accumulation of fat in the neck area is not normally part of any standardized assessment of human adipose tissue distribution, but a quantitative estimate of fat mass in the neck region is likely to be clinically relevant because of the number of adiposity redistribution conditions with severe metabolic complications such as familial partial lipodystrophy [3,4], Cushingoid syndromes [2] and obesity hypoventilation syndrome [5]. Here, we show that NFM can be reliably estimated using standard DEXA images in conjunction with machine

Table 3

SNPs previously associated with neck circumference or neck adiposity. RSID = Reference SNP cluster ID; REF = reference base; ALT = alternative base; MAF = minor allele frequency; OBB = Oxford BioBank.

RSID	Chromosome	Base Pair Position (HG19 genome build)	Closest Mapped Genes (flanking = 30 kb)	REF (OBB)	ALT (OBB)	MAF (OBB)	Study	Association
rs10244704	7	136,339,927	<i>LOC100507642</i>	C	T	0.139	Liu et al 2021 [41]	Neck circumference
rs11859825	16	53,325,073	<i>DDX11L10, MIR6859-1, MIR6859-2, RAB11FIP3, CHD9</i>	C	A	0.000	Davies et al 2013 [40]	Neck adiposity, neck circumference
rs12422456	12	43,986,076	<i>FAM138D, KDM5A, CCND2</i>	A	C	0.098	Liu et al 2021 [41]	Neck circumference
rs12647166	4	142,760,932	<i>NKX1-1</i>	A	T	0.433	Liu et al 2021 [41]	Neck circumference
rs12823146	12	95,937,604	<i>FAM138D, DDX12P, METAP2, USP44</i>	G	T	0.344	Liu et al 2021 [41]	Neck circumference
rs13087058	3	73,551,228	<i>LOC102723448, LINC01266, GRM7, PDZRN3</i>	T	C	0.393	Liu et al 2021 [41]	Neck circumference (BMI adjusted)
rs139177122	7	71,189,097	<i>PRKAR1B, LOC100131257, WBSCR17</i>	A	G	0.029	Liu et al 2021 [41]	Neck circumference
rs1421085	16	53,800,954	<i>DDX11L10, MIR6859-1, MIR6859-2, RAB11FIP3, FTO</i>	T	C	0.413	Tóth et al 2020 [39]	Neck adipocyte browning
rs1483197	1	4,770,904	<i>WASH7P, FAM138A, FAM138F, AJAP1, TAL1, STIL</i>	T	C	0.339	Liu et al 2021 [41]	Neck circumference
rs227724	17	54,778,817	<i>DOC2B, LOC100506371, VPS53, NLRP1</i>	A	T	0.343	Liu et al 2021 [41]	Neck circumference (BMI adjusted)
rs34342452	19	46,000,901	<i>SHC2, ODF3L2, FOSB, RTN2, PPM1N, VASP</i>	G	C	0.211	Liu et al 2021 [41]	Neck circumference
rs4606526	12	52,268,353	<i>FAM138D, KDM5A, CCDC77, ANKRD33</i>	A	G	0.105	Liu et al 2021 [41]	Neck circumference
rs56094641	16	53,806,453	<i>DDX11L10, MIR6859-1, MIR6859-2, RAB11FIP3, FTO</i>	A	G	0.413	Liu et al 2021 [41]	Neck circumference
rs7647178	3	73,565,183	<i>LOC102723448, LINC01266, GRM7, PDZRN3</i>	G	T	0.369	Liu et al 2021 [41]	Neck circumference

Table 4

SNPs associated with predicted neck parameters and corresponding findings from GWAS cohorts. RSID = Reference SNP cluster ID; REF = reference base; ALT = alternative base; MAF = minor allele frequency; OBB = Oxford BioBank; FDR = false discovery rate; ND = neck diameter; NC = neck circumference; NFMadjFM = neck adipose tissue mass adjusted to total body fat mass.

RSID	Association Coefficient	Standard Error	p value	p value FDR	Previous SNP Association	OBB SNP Association
rs12647166	0.045	0.021	0.0350000	0.1230	NC, women only, not BMI adjusted	ND, men and women
rs12647166	0.073	0.028	0.0090000	0.1260	NC, women only, not BMI adjusted	NAT _{adjFM} , women
rs12647166	0.064	0.028	0.0223000	0.1041	NC, women only, not BMI adjusted	ND, women
rs139177122	0.159	0.069	0.0200000	0.0930	NC, men only, not BMI adjusted	ND, men and women
rs56094641	0.085	0.021	0.0000742	0.0005	NC, men and women, not BMI adjusted	ND, men and women
rs56094641	0.071	0.021	0.0010000	0.0084	NC, men and women, not BMI adjusted	NFM, men and women
rs227724	−0.076	0.033	0.0231000	0.3234	NC, men and women, BMI adjusted	NAT _{adjFM} , men

learning tools. This was achieved by developing machine learning models that were trained to estimate either the NFM content or the neck ROI co-ordinates (to give ND values).

When comparing estimated NFM and ND with real measured values for NC and skinfold, we saw strong positive correlations. Our genetic analyses corroborated with existing data, confirming that the estimated measures of NFM were in accordance with existing studies. Interestingly, SNPs that had been previously associated with BMI-adjusted NC, were associated with NFMadjFM, as opposed to non-adjusted measures of neck adiposity, confirming the functionality of our adjustment protocols, and further indicating that these SNPs may pertain to specific NAT expansion, independent of body fat mass. One such SNP, rs227724, was the leading SNP in a study looking at NC [41], which highlighted the overlap of this SNP with an eQTL for the *NOG* gene, encoding the Noggin protein. Noggin expression has been shown to influence processes including cellular differentiation of adipose tissue, partly through interaction with BMP4 [42], which promoted white adipogenesis by inducing commitment of adipose precursors to the white adipocyte lineage [43,44]. Still, how these SNPs relate to total upper-body adiposity and metabolic risk is unclear and warrants further exploration. Subsequent studies looking at DEXA scans in larger cohorts, such as the UK BioBank (n > 70,000), would be of benefit to assess NFM, as this

would give the necessary power to conduct a full GWAS for NFM and NFMadjFM.

Understanding the relationship between NFM and the mass of other fat depots is essential to comprehensively assess the role of regional adiposity in cardiometabolic health. Fat distribution, independent of total fat mass, is an important determinant of metabolic health, with upper-body adiposity, particularly in the abdominal visceral compartment, being associated with adverse metabolic signatures [45], while lower-body adipose tissue accumulation appears protective [46]. NFM notably associated with abdominal adiposity, although when controlling for total body fat, we found that this positive relationship only held true for VFM and not subcutaneous adipose tissue (SAT). In agreement with this, longitudinal data has suggested that increases in NC are accompanied by increases in VAT to a greater extent than SAT [47]. This interesting relationship between NFM and VFM may be a product of shared developmental origins or functional properties. Linkage between NAT and VAT is evident in inherited lipodystrophies, such as the Dunnigan type familial partial lipodystrophy, where mutations in the Lamin A/C gene are specifically associated with the maintenance of visceral, neck and facial adipose tissues, concurrent with the loss of SAT [48]. Both NAT and VAT are also more responsive to glucocorticoids [48–50] and may produce more cortisol [51], compared to subcutaneous depots,

as seen in Cushing's disease, where hypercortisolism accompanies notable neck and visceral adiposity in conjunction with reduced SAT mass [2,48].

NFMadjFM and VFM were higher in individuals with T2DM and higher in men compared to women, implying that there is a shift in fat distribution, favouring NFM, dependent on both sex and metabolic status. Sex-dependent differences may result from steroid hormone responses; SAT is more oestradiol responsive compared to NAT and VAT [49]. Thus, in pre-menopausal women, where oestradiol levels are comparatively higher than in men, SAT expansion is favoured over VAT and NAT expansion. These effects may be further augmented by the sexual dimorphism in glucocorticoid responses; males may show heightened transcriptional responses to glucocorticoids [52], and also site-dependent differences in adipose tissue expansion capacity following glucocorticoid exposure, as compared to females [53,54]. In mice, testosterone treatment increased corticosterone-induced adipocyte hypertrophy and BAT whitening [55], potentially due to sex hormone-mediated modulation of glucocorticoid receptors [56]. Thus, differences in sex hormone and cortisol responses may contribute to BAT whitening and subsequent enlargement of NFM [57]. This may further explain the higher NFM observed in T2DM, since T2DM has also been associated with higher cortisol secretion compared to healthy controls [58].

In light of the observed strong correlations between NFM and VFM, as well as the associations with T2DM, we explored the relationships between NFM, and a range of commonly used parameters that associate with obesity-related complications, such as hsCRP, plasma triglycerides, total/HDL cholesterol ratio, insulin resistance (HOMA-IR), systolic blood pressure, and markers of adipose tissue lipolysis (NEFA). The observed significant associations were in accordance with existing studies, which have highlighted the relationships between NC and metabolic, as well as inflammatory, markers [26]. These relationships paralleled those of VAT before correcting for total body fat mass, which is of relevance considering that VAT accumulation is a strong predictor for cardiometabolic outcome, as compared to SAT expansion [59–61]. When correcting for total fat mass, NFMadjFM showed weaker associations than VFMadjFM with the selected risk factors, showing that relative neck adiposity does not predict cardiometabolic biomarkers as well as relative visceral adiposity. Weaker associations between NFM and metabolic biomarkers after correcting for total adiposity likely reflect the strong relationship between NFM and total fat mass in this healthy population. Still, given that NFMadjFM was significantly higher in individuals with T2DM, it would be valuable to establish whether these relationships change in metabolic disease, where we see a notable increase in NFMadjFM. In the healthy population, the range of VFMadjFM values greatly exceeded that of NFMadjFM, and thus studies of NFMadjFM in a more varied cohort would be valuable for better establishing the associations between NFMadjFM and metabolic risk.

In an attempt to assess the overall impact of NFM on cardiovascular health, we used the QRISK3 algorithm to compare QRISK3 score across deciles of NFMadjFM. This showed a 2-fold greater risk of 10-year cardiovascular events when comparing the bottom with the top decile. Notably, this analysis was made after adjusting for total fat mass, thus relative neck adiposity is an independent predictor of cardiovascular disease risk. VFMadjFM was a better predictor, and showed strong associations with blood pressure, which was not the case for NFMadjFM, potentially explaining the steeper association with VFMadjFM deciles and QRISK3, as compared with NFMadjFM. Still, these results agree with current research depicting the associations between NC and cardiometabolic outcomes, particularly in relation to T2DM [11,14,15,20]. Here, however, we uniquely discover that neck adiposity is an independent contributor to cardiometabolic risk, highlighting its potential utility as a clinical predictor for cardiometabolic disease.

CRediT authorship contribution statement

Emily Cresswell: Conceptualization, Formal analysis, Investigation, Visualization, Writing – original draft, Writing – review & editing. **Nicolas Basty:** Data curation, Formal analysis, Methodology, Software, Writing – review & editing. **Naeimeh Atabaki Pasdar:** Data curation, Formal analysis, Investigation, Writing – review & editing. **Fredrik Karpe:** Conceptualization, Supervision, Writing – review & editing. **Katherine E. Pinnick:** Conceptualization, Supervision, Writing – review & editing.

Declaration of competing interest

The authors declare that they have no known competing financial interests or personal relationships that could have appeared to influence the work reported in this paper.

Data availability

Data will be made available on request.

Acknowledgements

EC is funded by The Oxford Kennedy MB PhD Programme. FK is supported by the BHF RG17/1/32663. NAP is funded by the Swedish Research Council, Sweden (VR - Avtals-ID: 2021-06714_3) as part of a postdoctoral fellowship and acknowledges support from the Henning och Johan Throne-Holsts Foundation. The graphical abstract was made in BioRender.com.

References

- [1] M.D. Jensen, Role of body fat distribution and the metabolic complications of obesity, *J. Clin. Endocrinol. Metab.* 93 (11 Suppl 1) (2008) S57–S63.
- [2] E.J. Ross, D.C. Lynch, Cushing's syndrome-killing disease: discriminatory value of signs and symptoms aiding early diagnosis, *Lancet* 2 (8299) (1982) 646–649.
- [3] A. Garg, Acquired and inherited lipodystrophies, *N. Engl. J. Med.* 350 (12) (2004) 1220–1234.
- [4] A. Garg, Lipodystrophies: genetic and acquired body fat disorders, *J. Clin. Endocrinol. Metab.* 96 (11) (2011) 3313–3325.
- [5] S. Shetty, S. Parthasarathy, Obesity hypoventilation syndrome, *Curr Pulmonol Rep* 4 (1) (2015) 42–55.
- [6] H. Sacks, M.E. Symonds, Anatomical locations of human brown adipose tissue: functional relevance and implications in obesity and type 2 diabetes, *Diabetes* 62 (6) (2013) 1783–1790.
- [7] J. Nedergaard, T. Bengtsson, B. Cannon, Unexpected evidence for active brown adipose tissue in adult humans, *Am. J. Phys. Endocrinol. Metab.* 293 (2) (2007) E444–E452.
- [8] C. Pfannenberger, M.K. Werner, S. Ripkens, I. Stef, A. Deckert, M. Schmalz, et al., Impact of age on the relationships of brown adipose tissue with sex and adiposity in humans, *Diabetes* 59 (7) (2010) 1789–1793.
- [9] V. Ouellet, A. Routhier-Labadie, W. Bellemare, L. Lakhal-Chaieb, E. Turcotte, A. C. Carpentier, et al., Outdoor temperature, age, sex, body mass index, and diabetic status determine the prevalence, mass, and glucose-uptake activity of 18F-FDG-detected BAT in humans, *J. Clin. Endocrinol. Metab.* 96 (1) (2011) 192–199.
- [10] K. Joshipura, F. Munoz-Torres, J. Vergara, C. Palacios, C.M. Perez, Neck circumference may be a better alternative to standard anthropometric measures, *J. Diabetes Res.* 2016 (2016) 6058916.
- [11] L. Boemeke, F.V. Raimundo, M. Bopp, L.R. Leonhardt, S.A. Fernandes, C. A. Marroni, The correlation of neck circumference and insulin resistance in NAFLD patients, *Arq. Gastroenterol.* 56 (1) (2019) 28–33.
- [12] I. Ozkaya, A. Tuncakale, Neck circumference positively related with central obesity and overweight in Turkish university students: a preliminary study, *Cent. Eur. J. Public Health* 24 (2) (2016) 91–94.
- [13] Y. Luo, X. Ma, Y. Shen, Y. Xu, Q. Xiong, X. Zhang, et al., Neck circumference as an effective measure for identifying cardio-metabolic syndrome: a comparison with waist circumference, *Endocrine* 55 (3) (2017) 822–830.
- [14] S.R. Preis, J.M. Massaro, U. Hoffmann, R.B. D'Agostino Sr., D. Levy, S.J. Robins, et al., Neck circumference as a novel measure of cardiometabolic risk: the Framingham Heart study, *J. Clin. Endocrinol. Metab.* 95 (8) (2010) 3701–3710.
- [15] A.L. Borel, S. Coumes, F. Reche, S. Ruckly, J.L. Pepin, R. Tamisier, et al., Waist, neck circumferences, waist-to-hip ratio: which is the best cardiometabolic risk marker in women with severe obesity? the SOON cohort, *PLoS One* 13 (11) (2018) e0206617.
- [16] N.G. Vallianou, A.A. Evangelopoulos, V. Bountziouka, E.D. Vogiatzakis, M. S. Bonou, J. Barbetseas, et al., Neck circumference is correlated with triglycerides

- and inversely related with HDL cholesterol beyond BMI and waist circumference, *Diabetes Metab. Res. Rev.* 29 (1) (2013) 90–97.
- [17] C.D. Sjöström, A.C. Hakangård, L. Lissner, L. Sjöström, Body compartment and subcutaneous adipose tissue distribution—risk factor patterns in obese subjects, *Obes. Res.* 3 (1) (1995) 9–22.
 - [18] E. Valencia-Sosa, C. Chavez-Palencia, E. Romero-Velarde, A. Larrosa-Haro, E. M. Vasquez-Garibay, C.O. Ramos-Garcia, Neck circumference as an indicator of elevated central adiposity in children, *Public Health Nutr.* 22 (10) (2019) 1755–1761.
 - [19] M.S. Filgueiras, F.M. Albuquerque, A.P.P. Castro, N.P. Rocha, L.C. Milagres, J. F. Novaes, Neck circumference cutoff points to identify excess android fat, *J. Pediatr. (Rio J)* 96 (3) (2020) 356–363.
 - [20] A. Scovronec, A. Provencher, S. Iceta, M. Pelletier, V. Leblanc, M. Nadeau, et al., Neck circumference is a better correlate of insulin resistance markers than other standard anthropometric indices in patients presenting severe obesity, *Obes. Res. Clin. Pract.* 16 (4) (2022) 307–313.
 - [21] J.J. Lee, A. Pedley, K.E. Therkelsen, U. Hoffmann, J.M. Massaro, D. Levy, et al., Upper body subcutaneous fat is associated with cardiometabolic risk factors, *Am J Med* 130(8) (2017) 958–966 e1.
 - [22] N. Xia, H. Li, The role of perivascular adipose tissue in obesity-induced vascular dysfunction, *Br. J. Pharmacol.* 174 (20) (2017) 3425–3442.
 - [23] E.C. Eringa, W. Bakker, V.W. van Hinsbergh, Paracrine regulation of vascular tone, inflammation and insulin sensitivity by perivascular adipose tissue, *Vasc. Pharmacol.* 56 (5–6) (2012) 204–209.
 - [24] F. Fantin, G. Comellato, A.P. Rossi, E. Grison, E. Zoico, G. Mazzali, et al., Relationship between neck circumference, insulin resistance and arterial stiffness in overweight and obese subjects, *Eur. J. Prev. Cardiol.* 24 (14) (2017) 1532–1540.
 - [25] K.V. Fitch, T.L. Stanley, S.E. Looby, A.M. Rope, S.K. Grinspoon, Relationship between neck circumference and cardiometabolic parameters in HIV-infected and non-HIV-infected adults, *Diabetes Care* 34 (4) (2011) 1026–1031.
 - [26] M.J. Arias-Tellez, F.M. Acosta, Y. Garcia-Rivero, J.M. Pascual-Gamarra, E. Merchan-Ramirez, B. Martinez-Tellez, et al., Neck adipose tissue accumulation is associated with higher overall and central adiposity, a higher cardiometabolic risk, and a pro-inflammatory profile in young adults, *Int. J. Obes. (Lond)* 45 (4) (2021) 733–745.
 - [27] V. Pandzic Jaksic, D. Grizelj, A. Livun, D. Boscic, M. Ajduk, R. Kusec, et al., Neck adipose tissue - tying ties in metabolic disorders, *horm Mol biol, Clin. Investig.* 33 (2) (2018).
 - [28] M.L. Martin, M.D. Jensen, Effects of body fat distribution on regional lipolysis in obesity, *J. Clin. Invest.* 88 (2) (1991) 609–613.
 - [29] Z. Guo, D.D. Hensrud, C.M. Johnson, M.D. Jensen, Regional postprandial fatty acid metabolism in different obesity phenotypes, *Diabetes* 48 (8) (1999) 1586–1592.
 - [30] L.L.M. Santos, M. Diniz, A.C. Goulart, S.M. Barreto, R.C. Figueiredo, Association between neck circumference and non-alcoholic fatty liver disease: cross-sectional analysis from ELSA-brasil, *Sao Paulo Med J* 140 (2) (2022) 213–221.
 - [31] B.X. Huang, M.F. Zhu, T. Wu, J.Y. Zhou, Y. Liu, X.L. Chen, et al., Neck circumference, along with other anthropometric indices, has an independent and additional contribution in predicting fatty liver disease, *PLoS One* 10 (2) (2015) e0118071.
 - [32] M. Torriani, C.M. Gill, S. Daley, A.L. Oliveira, D.C. Azevedo, M.A. Bredella, Compartmental neck fat accumulation and its relation to cardiovascular risk and metabolic syndrome, *Am. J. Clin. Nutr.* 100 (5) (2014) 1244–1251.
 - [33] S. Tal, I. Litovchik, M.M. Klar, H.S. Maresky, N. Grysman, I. Wiser, et al., The association between neck adiposity and long-term outcome, *PLoS One* 14 (4) (2019) e0215538.
 - [34] D.R. Sarvamangala, R.V. Kulkarni, Convolutional neural networks in medical image understanding: a survey, *Evol. Intel.* 15 (1) (2022) 1–22.
 - [35] F. Karpe, S.K. Vasan, S.M. Humphreys, J. Miller, J. Cheeseman, A.L. Dennis, et al., Cohort profile: the Oxford biobank, *Int. J. Epidemiol.* 47 (1) (2018), 21–21g.
 - [36] E. Cresswell, F. Karpe, N. Bastý, Neck fat estimation from DXA using convolutional neural networks, *Lect Notes Comput Sc* 13413 (2022) 3–12.
 - [37] H. Peng, W. Gong, C.F. Beckmann, A. Vedaldi, S.M. Smith, Accurate brain age prediction with lightweight deep neural networks, *Med. Image Anal.* 68 (2021) 101871.
 - [38] J. Hippisley-Cox, C. Coupland, P. Brindle, Development and validation of QRISK3 risk prediction algorithms to estimate future risk of cardiovascular disease: prospective cohort study, *BMJ* 357 (2017) j2099.
 - [39] B.B. Toth, R. Arianti, A. Shaw, A. Vámos, Z. Vereb, S. Poliska, et al., FTO intronic SNP strongly influences human neck adipocyte browning determined by tissue and PPARgamma specific regulation: a transcriptome analysis, *Cells* 9 (4) (2020).
 - [40] R.W. Davies, P. Lau, T. Naing, M. Nikpay, H. Doelle, M.E. Harper, et al., A 680 kb duplication at the FTO locus in a kindred with obesity and a distinct body fat distribution, *Eur. J. Hum. Genet.* 21 (12) (2013) 1417–1422.
 - [41] Y. Liu, X. Zhang, J. Lee, D. Smelser, B. Cade, H. Chen, et al., Genome-wide association study of neck circumference identifies sex-specific loci independent of generalized adiposity, *Int. J. Obes. (Lond)* 45 (7) (2021) 1532–1541.
 - [42] C. Chen, J. Lin, L. Li, T. Zhu, L. Gao, W. Wu, et al., The role of the BMP4/Smad1 signaling pathway in mesangial cell proliferation: a possible mechanism of diabetic nephropathy, *Life Sci.* 220 (2019) 106–116.
 - [43] A.M. Blazquez-Medela, M. Jumabay, P. Rajbhandari, T. Sallam, Y. Guo, J. Yao, et al., Noggin depletion in adipocytes promotes obesity in mice, *Mol Metab* 25 (2019) 50–63.
 - [44] B. Gustafson, A. Hammarstedt, S. Hedjazifar, J.M. Hoffmann, P.A. Svensson, J. Grimsby, et al., BMP4 and BMP antagonists regulate human white and beige adipogenesis, *Diabetes* 64 (5) (2015) 1670–1681.
 - [45] N. Alexopoulos, D. Katritsis, P. Raggi, Visceral adipose tissue as a source of inflammation and promoter of atherosclerosis, *Atherosclerosis* 233 (1) (2014) 104–112.
 - [46] K.E. Pinnick, G. Nicholson, K.N. Manolopoulos, S.E. McQuaid, P. Valet, K.N. Frayn, et al., Distinct developmental profile of lower-body adipose tissue defines resistance against obesity-associated metabolic complications, *Diabetes* 63 (11) (2014) 3785–3797.
 - [47] W. Cao, Y. Xu, Y. Shen, T. Hu, Y. Xiao, Y. Wang, et al., Change of neck circumference in relation to visceral fat area: a chinese community-based longitudinal cohort study, *Int. J. Obes. (Lond)* 46 (9) (2022) 1633–1637.
 - [48] S. Gesta, Y.H. Tseng, C.R. Kahn, Developmental origin of fat: tracking obesity to its source, *Cell* 131 (2) (2007) 242–256.
 - [49] D.C. Berry, D. Stenese, D. Zeve, J.M. Graff, The developmental origins of adipose tissue, *Development* 140 (19) (2013) 3939–3949.
 - [50] M.J. Lee, P. Pramyothin, K. Karastergiou, S.K. Fried, Deconstructing the roles of glucocorticoids in adipose tissue biology and the development of central obesity, *Biochim. Biophys. Acta* 1842 (3) (2014) 473–481.
 - [51] I.J. Bujalska, S. Kumar, P.M. Stewart, Does central obesity reflect “Cushing’s disease of the omentum”? *Lancet* 349 (9060) (1997) 1210–1213.
 - [52] D. Duma, J.B. Collins, J.W. Chou, J.A. Cidlowski, Sexually dimorphic actions of glucocorticoids provide a link to inflammatory diseases with gender differences in prevalence, *Sci. Signal.* 3 (143) (2010) ra74.
 - [53] P.G. McTernan, L.A. Anderson, A.J. Anwar, M.C. Eggo, J. Crocker, A.H. Barnett, et al., Glucocorticoid regulation of p450 aromatase activity in human adipose tissue: gender and site differences, *J. Clin. Endocrinol. Metab.* 87 (3) (2002) 1327–1336.
 - [54] C.H. Bourke, C.S. Harrell, G.N. Neigh, Stress-induced sex differences: adaptations mediated by the glucocorticoid receptor, *Horm. Behav.* 62 (3) (2012) 210–218.
 - [55] S.J. Gasparini, M.M. Swarbrick, S. Kim, L.J. Thai, H. Henneicke, L.L. Cavanagh, et al., Androgens sensitise mice to glucocorticoid-induced insulin resistance and fat accumulation, *Diabetologia* 62 (8) (2019) 1463–1477.
 - [56] D.C.E. Spaanderman, M. Nixon, J.C. Buurstedde, H.C. Sips, M. Schilperoord, E. N. Kuipers, et al., Androgens modulate glucocorticoid receptor activity in adipose tissue and liver, *J. Endocrinol.* (2018).
 - [57] L.E. Ramage, M. Akyol, A.M. Fletcher, J. Forsythe, M. Nixon, R.N. Carter, et al., Glucocorticoids acutely increase brown adipose tissue activity in humans, revealing species-specific differences in UCP-1 regulation, *Cell Metab.* 24 (1) (2016) 130–141.
 - [58] I. Chiodini, G. Adda, A. Scillitani, F. Coletti, V. Morelli, S. Di Lembo, et al., Cortisol secretion in patients with type 2 diabetes: relationship with chronic complications, *Diabetes Care* 30 (1) (2007) 83–88.
 - [59] T. Hayashi, E.J. Boyko, D.L. Leonetti, M.J. McNeely, L. Newell-Morris, S.E. Kahn, et al., Visceral adiposity is an independent predictor of incident hypertension in Japanese Americans, *Ann. Intern. Med.* 140 (12) (2004) 992–1000.
 - [60] I.J. Neeland, R. Ross, J.P. Despres, Y. Matsuzawa, S. Yamashita, I. Shai, et al., Visceral and ectopic fat, atherosclerosis, and cardiometabolic disease: a position statement, *Lancet Diabetes Endocrinol.* 7 (9) (2019) 715–725.
 - [61] E.J. Boyko, W.Y. Fujimoto, D.L. Leonetti, L. Newell-Morris, Visceral adiposity and risk of type 2 diabetes: a prospective study among Japanese Americans, *Diabetes Care* 23 (4) (2000) 465–471.